

Structure, electronic, and nonlinear optical properties of superalkaline M_3O (M=Li, Na) doped cyclo[18]carbon

Xiao-Dong Liu(刘晓东), Qi-Liang Lu(卢其亮), and Qi-Quan Luo(罗其全)
Citation: Chin. Phys. B, 2024, 33 (**2**): 023601. DOI: 10.1088/1674-1056/ace036
Journal homepage: http://cpb.iphy.ac.cn; http://iopscience.iop.org/cpb

What follows is a list of articles you may be interested in

Single-electron transport in $H_2O@C_{60}$ single-molecule transistors

Bowen Liu(刘博文), Jun Chen(陈俊), Yiping Ouyang(欧阳一平), Minhao Zhang(张敏昊), Yuan-Zhi Tan(谭元植), and Fengqi Song(宋凤麒)
Chin. Phys. B, 2023, 32 (**6**): 063601. DOI: 10.1088/1674-1056/acc801

Density functional study on the bimetallic Ti_mZr_n (n+m ≤ 5) clusters and their interactions with H_2

Ge Zhang(张鸽), Yong Sheng(盛勇)
Chin. Phys. B, 2018, 27 (**9**): 093601. DOI: 10.1088/1674-1056/27/9/093601

Effect of Ni and vacancy concentration on initial formation of Cu precipitate in Fe-Cu-Ni ternary alloys by molecular dynamics simulation

Ke Liu(刘珂), Li-Juan Hu(胡丽娟), Qiao-Feng Zhang(张巧凤), Yao-Ping Xie(谢耀平), Chao Gao(高超), Hai-Ying Dong(董海英), Wan-Yi Liang(梁婉怡)
Chin. Phys. B, 2017, 26 (**8**): 083601. DOI: 10.1088/1674-1056/26/8/083601

Structural optimization of Au-Pd bimetallic nanoparticles with improved particle swarm optimization method

Gui-Fang Shao(邵桂芳), Meng Zhu(朱梦), Ya-Li Shangguan(上官亚力), Wen-Ran Li(李文然), Can Zhang(张灿), Wei-Wei Wang(王玮玮), Ling Li(李玲)
Chin. Phys. B, 2017, 26 (**6**): 063601. DOI: 10.1088/1674-1056/26/6/063601

Influence of Ni on Cu precipitation in Fe–Cu–Ni ternary alloy by an atomic study

Zhu Lu-Shan (朱露珊), Zhao Shi-Jin (赵世金)
Chin. Phys. B, 2014, 23 (**6**): 063601. DOI: 10.1088/1674-1056/23/6/063601

Structure, electronic, and nonlinear optical properties of superalkaline M_3O (M = Li, Na) doped cyclo[18]carbon

Xiao-Dong Liu(刘晓东)[1], Qi-Liang Lu(卢其亮)[1,†], and Qi-Quan Luo(罗其全)[2,3]

[1] *School of Physics and Material Science, Anhui University, Hefei* 230601, *China*
[2] *Institute of Physical Science and Information Technology, Anhui University, Hefei* 230601, *China*
[3] *Department of Chemical Physics, University of Science and Technology of China, Hefei* 230026, *China*

(Received 18 April 2023; revised manuscript received 4 June 2023; accepted manuscript online 21 June 2023)

Cyclo[18]carbon has received considerable attention thanks to its novel geometric configuration and special electronic structure. Superalkalis have low ionization energy. Doping a superalkali in cyclo[18]carbon is an effective method to improve the optical properties of the system because considerable electron transfer occurs. In this paper, the geometry, bonding properties, electronic structure, absorption spectrum, and nonlinear optical (NLO) properties of superalkaline M_3O (M = Li, Na)-doped cyclo[18]carbon were studied by using density functional theory. M_3O and the C_{18} rings are not coplanar. The C_{18} ring still exhibits alternating long and short bonds. The charge transfer between M_3O and C_{18} forms stable $[M_3O]^+[C_{18}]^-$ ionic complexes. $C_{18}M_3O$ (M = Li, Na) shows striking optical nonlinearity, i.e., their first- and second-order hyperpolarizability (β_{vec} and $\gamma_{||}$) increase considerably at λ = 1907 nm and 1460 nm.

Keywords: superalkaline doped cyclo[18]carbon, structure and electronic properties, nonlinear optical properties, density functional theory (DFT)

PACS: 36.40.–c, 36.40.Vz **DOI:** 10.1088/1674-1056/ace036

1. Introduction

Carbon has long been a popular research topic. In 1985, Kroto *et al*. obtained sp-hybridized fullerene C_{60} clusters[1] with a coordination number of three by laser vaporization. This result opened a new door for the study of low-dimensional materials. Since then, carbon nanotubes[2] and graphene[3] have been synthesized successively, and the family of molecular carbon allotropes has continued to expand. In 1966, Hoffman proposed the ring-like C_{18} cluster.[4] Since the first detection of the C_{18} ring in 1989,[5] small carbon clusters have attracted extensive attention from experimental and theoretical studies.[5–8] One of the most impressive advances in this field in recent years is the successful synthesis and characterization of a ring consisting of 18 carbon atoms, named cyclo[18]carbon, on the surface of Cu(111) by Kaiser *et al*.[9] Recently, Anderson *et al*.[10] proposed an efficient synthesis of C_{18} from bromocyclic carbon ($C_{18}Br_6$). This discovery has attracted the extensive attention of scholars who wish to study cyclic[n]carbon, and its analogs and derivatives due to its potential use in practical applications.[11–36] Many studies have shown that the C–C bond of the most stable structure of C_{18} cannot be simply described as alternating single and triple bonds but can only be described as alternating long and short bonds.[9,14,16,19]

The diameter of cyclo[18]carbon is about 7.40 Å,[17] which is equivalent to the size of C_{60} (7.1 Å). Cyclo[18]carbon provides sufficient space to encapsulate a range of other atoms or small molecules, thus forming a similar endohedral fullerene species.[37–40] This endohedral complex is an interesting structure from the perspective of research and application. Compared with many studies on the structure and properties of cyclo[18]carbon, work on the structure and properties of doped C_{18}[41–49] and other carbon rings[50–53] is limited. Alkali metal atoms have the lowest ionization energy (5.39 eV–3.89 eV) in the periodic table.[54] However, some polyatomic molecules or clusters, which are called "superalkali" by Gutsev and Boldyrev,[55] have lower ionization energies than cesium atoms (3.89 eV).[54] Studies have also shown the formation of an electron donor–acceptor endohedral complex with superalkali inside C_{60}[56] and $Si_{12}C_{12}$[57] nanocage. Their nonlinear optical properties are significantly improved. Liu *et al*.[29] systematically studied the electronic structure, electronic spectra, and optical nonlinearity of cyclo[18]carbon. They also investigated the properties of the Li@C_{18} complex and its potential application in an optical molecular switch.[43] It has also been shown that C_{18} molecules have strong electron acceptor properties.[33] Therefore, stable complexes can form between C_{18} and electron donor species, which implies a strong capability of charge transfer within complexes and excellent optical properties. Therefore, investigating the structure and properties of superalkali-doped C_{18} is worthwhile. In this work, we report systematic theoretical studies on the structure and properties of superalkaline M_3O (M = Li, Na)-doped cyclo[18]carbons.

[†]Corresponding author. E-mail: qllufd@vip.sina.com

© 2024 Chinese Physical Society and IOP Publishing Ltd

2. Computational methods

An extensive structural search for $C_{18}M_3O$ (M = Li, Na) was conducted based on the two low-energy isomers of cyclo[18]carbon; namely, the alternating bond length structure and the transition state structure with equal bond length.[9,14,16,19] Superalkaline molecules M_3O (M = Li, Na) were placed on the inner/outer edges of the ring and in different regions above the ring. Geometry optimization was performed at the M06-2X/def2-TZVP level for these different initial structures by using the Gaussian 09 software package.[58] Single-point energy calculations were performed at the CCSD(T)/def2-TZVP level to confirm the lowest energy structure. Vibrational frequency analyses were conducted on optimized structures to determine whether they are at the minimum or saddle point on the potential energy surface. Zero-point energy and the counterpoise procedure for basis set superposition error (BSSE) were utilized to calculate energies. On the basis of the results of Gaussian 09, Mayer bond order[59–61] and localized orbital locator (LOL) analysis[62–64] were performed using Multiwfn 3.8.[65] Electrostatic potential (ESP) analysis was performed using Visual Molecular Dynamics (VMD) software[66] in combination with Multiwfn. Meanwhile, ωB97XD is reliable and robust for studying photophysical properties and optical nonlinearity of C_{18} molecule and its analogs.[29,34,43,46] Therefore, ωB97XD is considered to be capable of describing the optical properties of the $C_{18}M_3O$ system. Electron excitations were studied by using the time-dependent density functional theory (TD-DFT) method at the ωB97XD/def2-TZVP level. Charge-transfer spectra (CTS) were plotted based on the results of TD-DFT.[58] The (hyper)polarizability of $C_{18}M_3O$ complex was calculated by coupled-perturbed Kohn–Sham (CPKS) method at the ωB97XD/aug-cc-pVTZ level.[46,67–70] Polarizability, the first hyperpolarizability, and the second hyperpolarizability were analyzed by Multiwfn and VMD. For the parameters of describing the nonlinear optical properties, we follow the formulas for calculating the response properties to electric field provided in Refs. [34,43].

3. Results and discussion

The most stable structures of $C_{18}M_3O$ (M = Li, Na) are shown in Fig. 1. Compared with the isolated cyclo[18]carbon, the C_{18} ring in $C_{18}Na_3O$ has higher structural deformation than that in $C_{18}Li_3O$. The M_3O moiety is not entrapped in the cyclo[18]carbon and is located some distance above the carbon ring. For $C_{18}Li_3O$, the distance between O atom and the center of C_{18} is about 0.99 Å. The projection of the oxygen atom on the C_{18} plane is almost located in the geometric center of the optimized C_{18} ring. However, for $C_{18}Na_3O$, the projection of the oxygen atom deviates far from the point. The four atoms of the Li_3O moiety are no longer coplanar and three Li atoms are close to the C_{18} ring. This finding may be attributed to the attraction between Li atoms and C_{18} ring resulting from charge transfer, as discussed later on. The Li_3 plane is almost parallel to the C_{18} plane. For $C_{18}Na_3O$, the Na_3 plane is at an angle to the C_{18} plane. The three shortest distances of Li–C are in the range from 2.24 Å to 2.27 Å. The values of Na–C are in the range from 2.62 Å to 2.68 Å.

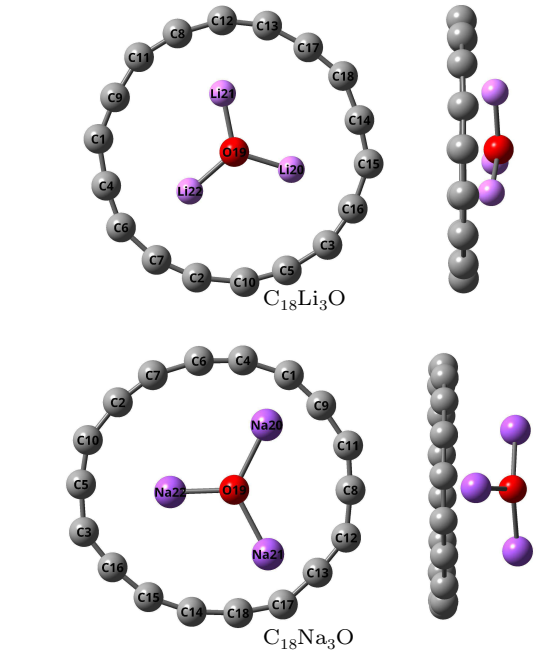


Fig. 1. Top and side views of the structure of $C_{18}M_3O$ (M = Li, Na).

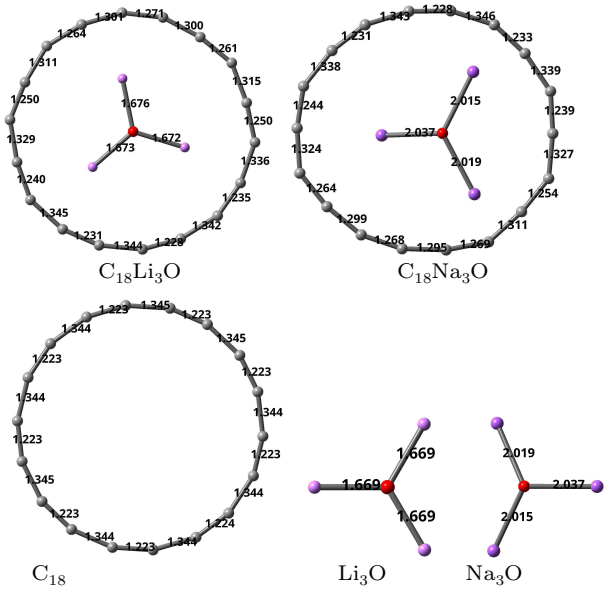


Fig. 2. Bond lengths (Å) of $C_{18}Li_3O$ and $C_{18}Na_3O$. The lengths of pristine C_{18}, Li_3O and Na_3O are given for comparison.

Alternating C–C bond lengths (Fig. 2) are also found in $C_{18}Li_3O$ and $C_{18}Na_3O$. The C–C bond lengths of the isolated cyclo[18]carbon are 1.223 Å and 1.344 Å at the present level of theory. Compared with the values of the pristine C_{18} ring,

$C_{18}M_3O$ has short C–C bonds that become shorter and long C–C bonds that become longer. Little difference can be found between the M–O bond length of $C_{18}M_3O$ and the free-state M_3O.

The binding energy (E_b) of M_3O to C_{18} ring can be defined as follows:

$$-E_b = E(C_{18}M_3O) - E(C_{18}) - E(M_3O),$$

where $E(C_{18}M_3O)$ represents the energy of the most stable structure of $C_{18}M_3O$. $E(C_{18})$ and $E(M_3O)$ represent the single-point energies of C_{18} and M_3O moieties, respectively, based on the ground-state structure of $C_{18}M_3O$. The obtained E_b values of Li_3O and Na_3O are 3.675 eV and 3.315 eV, respectively. Large binding energies suggest strong interactions between M_3O and the C_{18} ring.

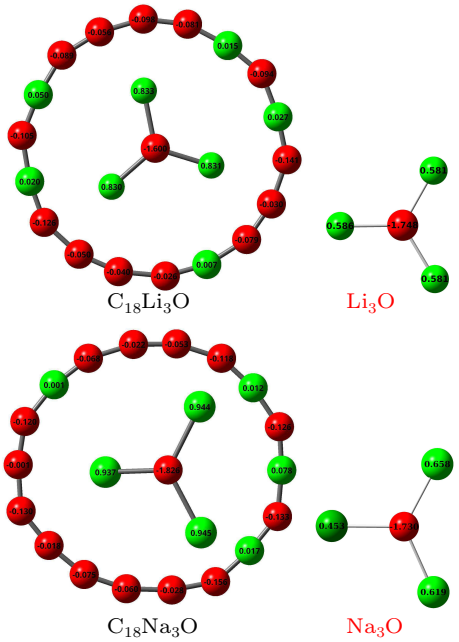


Fig. 3. Natural charge populations of $C_{18}Li_3O$ and $C_{18}Na_3O$. The values of isolated Li_3O and Na_3O are given for comparison.

The calculated natural charge populations of $C_{18}Li_3O$ and $C_{18}Na_3O$ are shown in Fig. 3. Their charge transfers are similar. The oxygen atom and C_{18} ring are negatively charged, whereas alkali atoms lose electrons. The oxygen atom obtains about two-thirds of the transferred electrons. The remaining one-third of the transferred electrons are transferred to cyclo[18]carbon, resulting in a negatively charged ring. The C_{18} ring obtains about 0.9e and 1.0e charges from Li_3O and Na_3O, respectively. The charge transfer between M_3O and C_{18} forms stable $[M_3O]^+[C_{18}]^-$ ionic complexes. This result supports the previous statement that the C_{18} molecule is a good electron acceptor.[33] Na atoms lose more electrons than Li atoms do. The negative charges are not evenly distributed on carbon atoms of the C_{18} ring. Few carbon atoms located far away from Li and Na carry a positive charge of no more than 0.08e. Other atoms near alkali atoms are negatively charged. The three M atoms possess almost identical charges in $C_{18}M_3O$. However, for isolated M_3O, significant differences can be found between Li_3O and Na_3O. The charges are evenly distributed on Li atoms. However, the number of charges of the two Na atoms is remarkably larger than that of the other Na atom. This finding indicates that the charge redistribution of Na_3O is greater than that of the Li_3O after doping into cyclo[18]carbon.

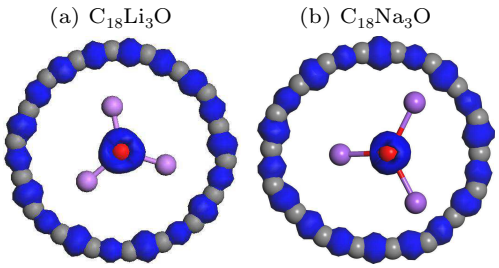


Fig. 4. Deformation electron densities of $C_{18}Li_3O$ and $C_{18}Na_3O$ (isovalue = 0.15|e|).

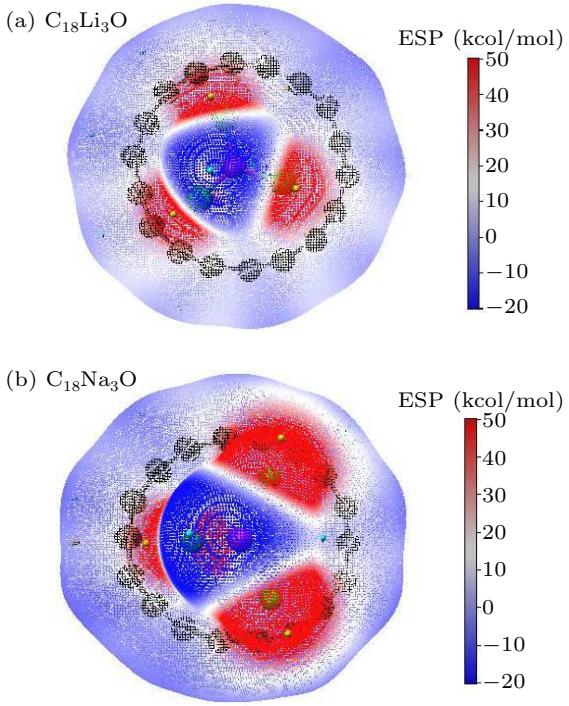


Fig. 5. Isosurface maps of the ESP for $C_{18}Li_3O$ and $C_{18}Na_3O$. Red and blue colors correspond to positive and negative parts of ESP, respectively.

The deformation electron density of $C_{18}M_3O$ is shown in Fig. 4. A large number of electrons are predominantly distributed in two carbon atoms of the C_{18} ring, indicating the covalent characteristics of the C–C bond. The alternating electron density also reveals the alternating bond strength between two carbon atoms, which is consistent with the analysis of bond length. Many electrons are distributed around the oxygen atom, indicating the existence of an ionic chemical bonding between alkali and oxygen atoms. This observation is confirmed by the result of natural charge population analysis. The

charge transfer from M_3O to C_{18} results in an electric field between the two moieties. ESP analysis[71] is an effective tool to understand the interaction between M_3O (M = Li, Na) and C_{18}. On the basis of the ESP map in Fig. 5, the regions around alkali atoms are positive ESP, whereas the circular regions surrounding the C_{18} ring and oxygen atom show negative values. The maximum ESP is near the alkali atoms, whereas the minimum ESP appears near the oxygen atom. Several local potential minimum points are distributed on the periphery of the C_{18} ring. The distribution pattern of ESP sufficiently reflects intermolecular electrostatic interaction between M_3O and C_{18}.

Figure 6 shows the Mayer bond order of $C_{18}Li_3O$ and $C_{18}Na_3O$ to further reveal the nature of the M_3O–C_{18} interaction and the bonding situation in the system. The bond orders between O and alkali atoms are no more than 0.41, indicating that the O–M covalent bond does not exist. This finding also confirms the results of population analysis and deformation electron density sections. The bond orders of C–M are less than 0.08, indicating that the chemical bond does not exist. This result probably occurred because the transferred electrons from M_3O are decentralized on other carbon atoms (Fig. 3). The C_{18} ring still exhibits alternating C–C bond orders. Most short bonds roughly satisfy double bonds, except for some bonds that deviate from 2.0. The orders of all long C–C bonds are larger than those of pristine cyclo[18]carbon.[16]

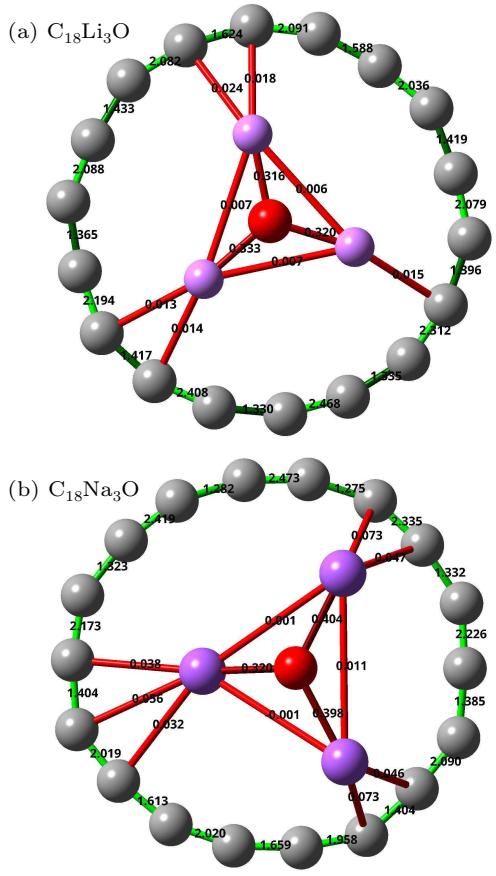


Fig. 6. Mayer bond orders of $C_{18}Li_3O$ and $C_{18}Na_3O$.

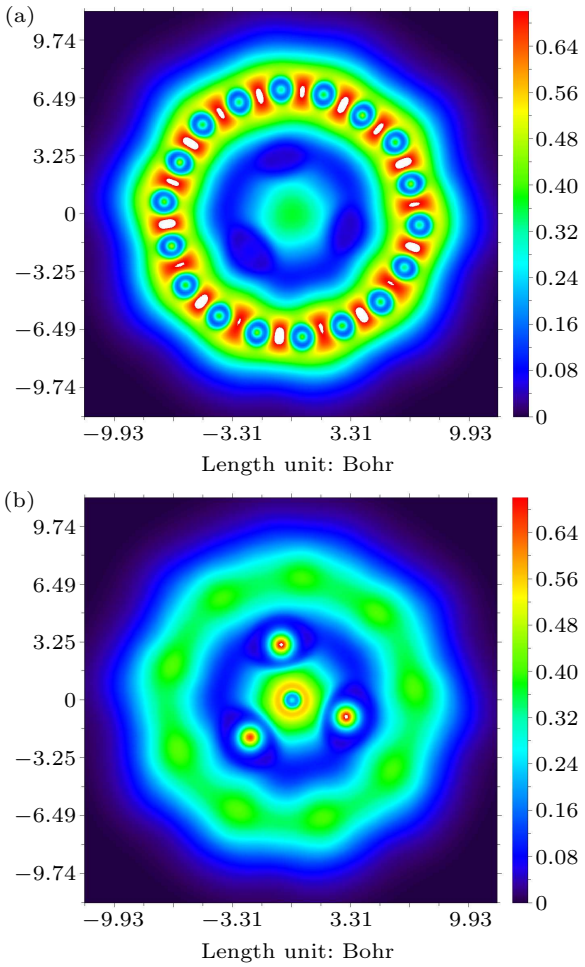


Fig. 7. The localized orbital locator of $C_{18}Li_3O$.

The LOL has useful real space functions in the range of 0–1 to unravel the delocalization of π electrons of the system. Given that the two planes of C_{18} ring and Li_3 moiety are almost parallel to each other, only the color-fill mapped LOL of $C_{18}Li_3O$ is shown in Fig. 7. Vast regions between Li_3O and C_{18} ring have LOL values much smaller than 0.5, indicating the absence of covalent bonds. We discussed earlier that they bind together by electrostatic attraction. A large LOL value (> 0.5) in the middle of the C–C bond indicates a strong covalent bond and exhibits alternating characteristics. The regions of the short C–C bonds are evidently broader than those of the long C–C bond. This result indicates that the π-electron delocalization of long C–C bonds is more difficult than that of short ones. Figure 7(b) shows the LOL–π map of the Li_3O at 1.4 Bohr above the C_{18} ring plane. Regions with a value larger than 0.5 are spherically distributed around the O atom. The values in the middle of the O–Li are small. These results further reveal that the O–M is not a covalent bond but an ionic bond. LOL based on π molecular orbitals can reflect the delocalization of π electrons in $C_{18}M_3O$ (Fig. S1). The inside isosurface of the C_{18} ring is broader than the outside ones for in-plane occupied π molecular orbitals, indicating that the delocalization over the π region inside the ring occurred some-

what easily. The out-of-plane orbitals centering on M_3O are not perpendicular to C_{18} ring; instead, they tilt outward the C_{18} ring slightly.

The electronic absorption spectrum can reflect electronic transition behavior in the $C_{18}M_3O$ system. As observed from Fig. 8, three absorption peaks exist for $C_{18}Li_3O$, in which two peaks are located at about 430 nm and 720 nm in the visible light region. The other one is a weak absorption at about 970 nm in the far infrared region. The spectrum of $C_{18}Na_3O$ is different from that of $C_{18}Li_3O$, showing two absorption peaks at about 424 nm and 725 nm. The absorption range of the $C_{18}Li_3O$ is wider than that of the $C_{18}Na_3O$, but its absorption intensity is much weaker than that of the latter.

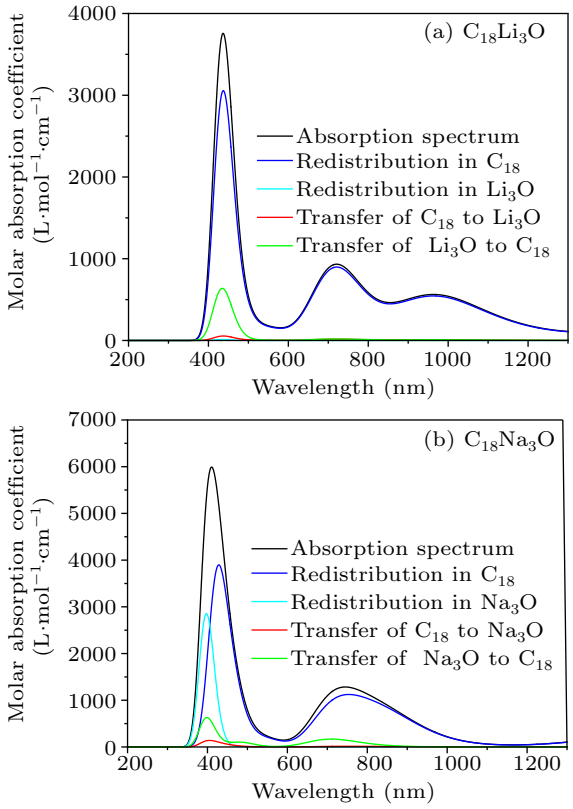


Fig. 8. Simulated absorption spectra and charge-transfer spectra of $C_{18}Li_3O$ and $C_{18}Na_3O$. Gaussian broaden for the full width at half-maximum (FWHM) of 2800 cm^{-1} was employed.

Lu *et al*. proposed a concept called CTS [43,46] to further reveal the nature of electron excitation from the charge redistribution within the fragment and charge transfer between two fragments of C_{18} moiety and M_3O. It can graphically present the contribution of charge redistribution. The colored CTSs are shown in Fig. 8. For $C_{18}Li_3O$, the contribution for the electron excitation overwhelmingly originates from the electron redistribution inside the C_{18} moiety, while the contribution of Li_3O group is almost negligible. The electron transfers from Li_3O to C_{18} have a significant proportion. In contrast, the nature of electron excitation of $C_{18}Na_3O$ is different from that of the $C_{18}Li_3O$ because many excitations of the former in the range of 340 nm–470 nm originate from the electron redistribution inside the Na_3O. The contribution of electron transfers from Na_3O to C_{18} to the absorption spectrum is also non-negligible.

Hole–electron analysis can intuitively reveal the excitation characteristics of electrons in a system.[29] The isosurface maps of hole and electron distributions related to their maximum absorptions of $C_{18}Li_3O$ and $C_{18}Na_3O$ are collectively given in the supplementary material (Fig. S2). As discussed earlier, the charges of three Na atoms are not equal before Na_3O doping into cyclo[18]carbon. The charge transfer within the Na_3O (charge redistribution) results in hole and electron distributions. Figure S2 shows that the absorption peak (397 nm) that corresponds to electron excitation (S0 $\rightarrow$ S47) originates from electron redistribution inside the Na_3O. This situation is not observed for $C_{18}Li_3O$. Thus, $C_{18}Na_3O$ and $C_{18}Li_3O$ have different electron excitations.

Polarizability and hyperpolarizability are the response characteristics of a molecule to an external electric field. Polarizability reflects the change in the dipole moment caused by applying one unit of electric field and hyperpolarizability represents the nonlinear polarization effect. Table 1 shows the calculated isotropic average polarizability (α_{iso}), the projection of the first hyperpolarizability on the molecular dipole (β_{vec}), and the average of the second hyperpolarizability ($\gamma_{||}$) of $C_{18}M_3O$ (M = Li, Na) under electric fields at different frequencies ($\lambda = \infty$; 1907 nm and 1460 nm). The calculated static and dynamic (hyper)polarizability of free C_{18} ring at the present theory level are given in the table. The corresponding results of Ref. [29] are also listed for comparison. Our results are very close to those of Ref. [29]. The $\alpha_{iso}(\infty)$ values of $C_{18}M_3O$ (M = Li, Na) are 1.20 and 1.25 times that of the free C_{18} ring (293.9 a.u.).[29] The β_{vec} of the cyclo[18]carbon is zero due to its the centrosymmetric structure. However, the introduction of M_3O causes a considerable magnitude of static β_{vec}. $C_{18}Li_3O$ and $C_{18}Na_3O$ present a larger static $\gamma_{||}$ ($\lambda = \infty$) than the pristine C_{18} ring (140909 a.u.).[29]

No significant difference is observed between static and dynamic polarizability (α_{iso}). α_{iso} changes slightly with frequency. Table 1 shows that the hyperpolarizability values (β_{vec} and $\gamma_{||}$) for $C_{18}Li_3O$ decrease rapidly with the frequency of the external electric field. At λ = 1907 nm and 1460 nm, $C_{18}Li_3O$ has $\gamma_{||}$ values of 115 and 5.8 times, respectively, which are higher than those of pristine C_{18} ring.[29] The β_{vec} values are 32.4 and 2.8 times, respectively, and the $\gamma_{||}$ values are 14.6 and 4.7 times, respectively, which are as much as the static values at the two frequencies. $C_{18}Na_3O$ also exhibits a strong polarization resonance effect under the dynamic external field at a low frequency because β_{vec} is 46 and 47 times higher, and $\gamma_{||}$ is 723 and 21 times higher than the static values at λ = 1907 nm and 1460 nm, respectively.

Table 1. Polarizabilities, the first- and the second-order hyperpolarizabilities (in a.u.) of $C_{18}Li_3O$, $C_{18}Na_3O$, and free C_{18} ring in zero-frequency limit case ($\lambda = \infty$) and frequency-dependent case (λ = 1907 nm and 1460 nm). The corresponding results of C_{18} of Ref. [29] are also listed.

Wavelength (nm)	∞	1907	1460
$(C_{18}Li_3O)\alpha_{iso}$	352.4	264.0	337.1
$(C_{18}Li_3O)\beta_{vec}$	−1678.9	−54458.0	−4830.4
$(C_{18}Li_3O)\gamma_{\|\|}$	−1266236	18555430	5988190
$(C_{18}Na_3O)\alpha_{iso}$	367.6	445.3	345.5
$(C_{18}Na_3O)\beta_{vec}$	1544.7	−71436.3	−72869.4
$(C_{18}Na_3O)\gamma_{\|\|}$	200122	144760100	−4267759
$(C_{18})\alpha_{iso}$	296.0 293.9[29]	298.7 296.6[29]	300.6 298.5[29]
$(C_{18})\beta_{vec}$	0 0[29]	0 0[29]	0 0[29]
$(C_{18})\gamma_{\|\|}$	142177 140909[29]	164099 161597[29]	178416 175625[29]

Some values of β_{vec} and $\gamma_{||}$ are negative. Lu *et al*. explained the meaning and the reason for their different signs.[43] The molecular volume is defined as the area surrounded by the electron density isosurface and has a close positive correlation with polarizability. This conclusion is also basically applicable to different types of molecules.[72] Therefore, the positive and negative signs of β_{xxx} and γ_{xxxx} can be attributed to whether the molecular volume increases or decreases when the electric field is applied, which turns the problem into how the electric field affects the electronic structure of the system. The external electric field can affect the electron distribution of molecules. As a result, the effective volume of electron density changes, and polarizability also changes.[43]

The unit sphere representation of (hyper)polarizability can be used to visualize and comprehensively characterize the (hyper)polarizability tensor,[73] and can intuitively reflect the molecular global and local features of response properties. Figure 9 shows the unit sphere representation of (hyper)polarizability of $C_{18}M_3O$ (M = Li, Na) under the electrostatic field. The molecular plane of C_{18} ring is set as the xy-plane. The (hyper)polarizability of $C_{18}M_3O$ (M = Li, Na) in the electrostatic field exhibits evident anisotropy. The x- and y- components of polarizability on the molecular plane are evidently larger than the component in the vertical direction (z-component). However, the z-component cannot be ignored because of dipole moments that result from the charge transfer between the C_{18} ring and M_3O. The tensor of all (hyper)polarizability suggests that some vector distributions (blue arrow) are perpendicular to the C_{18} plane, indicating that the response of (hyper)polarizability in this direction is not negligible. $C_{18}Li_3O$ and $C_{18}Na_3O$ exhibit similar characteristics of first-order hyperpolarizability tensors. Their x- and z-components are zero and have vanished in Figs. 9(b) and 9(e). However, a significant difference is observed in terms of the second-order hyperpolarizability. The x-component of $C_{18}Li_3O$ is remarkably larger than that of $C_{18}Na_3O$. In contrast, the y- and z-components of $C_{18}Na_3O$ are much larger than those of $C_{18}Li_3O$. The two components of $C_{18}Li_3O$ are small and negligible.

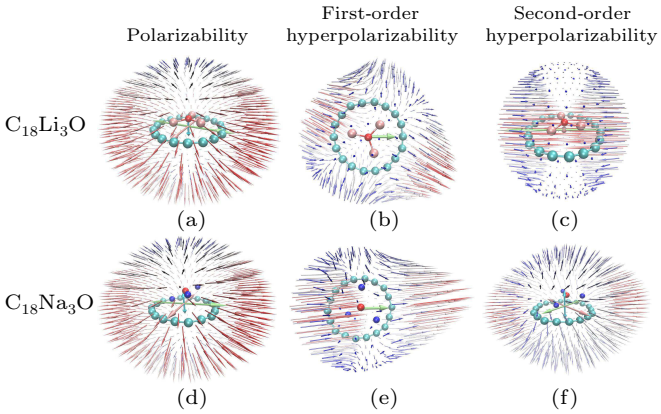


Fig. 9. Unit sphere representation of (hyper)polarizability for $C_{18}Li_3O$ and $C_{18}Na_3O$ in static electric field. The longer and redder arrow indicates a larger tensor value in the corresponding direction.

4. Conclusion

In this paper, we theoretically investigate the structural, electronic, electronic absorption spectrum, and nonlinear optical properties of M_3O (M = Li, Na)-doped cyclo[18]carbon. M_3O and the C_{18} ring are not coplanar. Alternating C–C bond lengths are found in the two complexes. The charge, electrostatic potential, bond order, and delocalization of π electrons are analyzed. Specifically, $C_{18}Li_3O$ and $C_{18}Na_3O$ show striking optical nonlinearity, i.e., their first- and second-order hyperpolarizability (β_{vec} and $\gamma_{||}$) increase significantly at λ = 1907 nm and 1460 nm. The relevant results are expected to provide theoretical guidance for the development of advanced cyclo[18]carbon-based functional molecules.

Acknowledgments

Project supported by the Natural Science Foundation of Anhui Province (Grant No. 1908085MA12) and the National Natural Science Foundation of China (Grant No. 21703222).

References

[1] Kroto H W, Heath J R, O'Brien S C, Curl R F and Smalley R E 1985 *Nature* **318** 162
[2] Iijima S 1991 *Nature* **354** 56
[3] Novoselov K S, Geim A K, Morozov S V, Jiang D, Zhang Y, Dubonos S V, Grigorieva I V and Firsov A A 2004 *Science* **306** 666
[4] Hoffmann R 1966 *Tetrahcdron* **22** 521
[5] Diederich F, Rubin Y, Knobler C B, Whetten R L, Schriver K E, Houk K N and Li Y 1989 *Science* **245** 1088
[6] Von Helden G, Gotts N G and Bowers M T 1993 *Nature* **363** 60
[7] Parasuk V, Almlof J and Feyereisen M W 1991 *J. Am. Chem. Soc.* **113** 1049
[8] Hutter J, Luethi H P and Diederich F 1994 *J. Am. Chem. Soc.* **116** 750
[9] Kaiser K, Scriven L M, Schulz F, Gawel P, Gross L and Anderson H L 2019 *Science* **365** 1299
[10] Scriven L M, Kaiser K, Schulz F, Sterling A J, Woltering S L, Gawel P, Christensen K E, Anderson H L and Gross L 2020 *J. Am. Chem. Soc.* **142** 12921

[11] Shi B, Yuan L, Tang T, Yuan Y and Tang Y 2020 *Chem. Phys. Lett.* **741** 136975
[12] Hussain S, Chen H, Zhang Z and Zheng H 2020 *Chem. Comm.* **56** 2336
[13] Li S X, Chen D L, Zhang Z P, Long Z W and Qin S J 2020 *Acta Phys. Sin.* **69** 103101 (in Chinese)
[14] Baryshnikov G V, Valiev R R, Kuklin A V, Sundholm D and Ågren H 2019 *J. Phys. Chem. Lett.* **10** 6701
[15] Fedik N, Kulichenko M, Steglenko D and Boldyrev A I 2020 *Chem. Comm.* **56** 2711
[16] Liu Z, Lu T and Chen Q 2020 *Carbon* **165** 468
[17] Li M, Gao Z, Han Y, Zhao Y, Yuan K, Nagase S, Ehara M and Zhao X 2020 *Phys. Chem. Chem. Phys.* **22** 4823
[18] Dai C, Chen D and Zhu J 2020 *Chem. Asian J.* **15** 2187
[19] Charistos N D and Muñoz-Castro A 2020 *Phys. Chem. Chem. Phys.* **22** 9240
[20] Nandi A, Solel E and Kozuch S 2020 *Chem. Eur. J.* **26** 625
[21] Brémond É, Pérez-Jiménez Á J, Adamo C and Sancho-García J C 2019 *J. Chem. Phys.* **151** 211104
[22] Zou W, Tao Y and Kraka E 2020 *J. Chem. Phys.* **152** 154107
[23] Hong I, Ahn J, Shin H, Bae H, Lee H, Benali A and Kwon Y 2020 *J. Phys. Chem. A* **124** 3636
[24] Fang S and Hu Y H 2021 *Carbon* **171** 96
[25] Zhang L, Li H, Feng Y P and Shen L 2020 *J. Phys. Chem. Lett.* **11** 2611
[26] Pereira Z S and da Silva E Z 2020 *J. Phys. Chem. A* **124** 1152
[27] Liang Z, He T, An J, Xue H, Tang F and Fan D 2020 *Int. J. Mod. Phys. B* **34** 2050138
[28] Jiang Y, Mattioli E J, Calvaresi M and Wang Z 2020 *Chem. Comm.* **56** 11835
[29] Liu Z, Lu T and Chen Q 2020 *Carbon* **165** 461
[30] Hou X, Ren Y, Fu F and Tian X 2020 *Comput. Theor. Chem.* **1187** 112922
[31] Baryshnikov G V, Valiev R R, Nasibullin R T, Sundholm D, Kurten T and Ågren H 2020 *J. Phys. Chem. A* **124** 10849
[32] Valiev R R, Baryshnikov G V, Nasibullin R T, Sundholm D and Ågren H 2020 *J. Phys. Chem. C* **124** 21027
[33] Stasyuk A J, Stasyuk O A, Solà M and Voityuk A A 2020 *Chem. Comm.* **56** 352
[34] Liu Z, Lu T, Yuan A, Wang X, Chen Q and Yan X 2021 *Chem Asian J* **16** 2267
[35] Liu Z, Lu T and Chen Q 2021 *Chem. Asian J.* **16** 56
[36] Lu T, Liu Z and Chen Q 2022 *Chin. Phys. B* **31** 126101
[37] Heath J, O'brien S, Zhang Q, Liu Y, Curl R, Tittel F and Smalley R 1985 *J. Am. Chem. Soc.* **107** 7779
[38] Wan Z, Christian J F and Anderson S L 1992 *Phys. Rev. Lett.* **69** 1352
[39] Kubozono Y, Maeda H, Takabayashi Y, Hiraoka K, Nakai T, Kashino S, Emura, S, Ukita S and Sogabe T 1996 *J. Am. Chem. Soc.* **118** 6998
[40] Thilgen C 2012 *Angew. Chem. Int. Ed.* **51** 587
[41] Liu Z, Lu T and Chen Q 2021 *Carbon* **171** 514
[42] Lu Q L, Ling Y and Luo Q Q 2022 *Chem. Phys. Lett.* **787** 139221
[43] Liu Z, Wang X, Lu T, Yuan A and Yan X 2022 *Carbon* **187** 78
[44] Zhao Q 2022 *J. Mol. Model.* **28** 210
[45] Chen J, Sun L and Zhang R 2021 *Phys. Chem. Chem. Phys.* **23** 17545
[46] Wang X, Liu Z, Yan X, Lu T, Wang H, Xiong W and Zhao M 2022 *Phys. Chem. Chem. Phys.* **24** 7466
[47] Ling Y, Lu Q L and Luo Q Q 2021 *Eur. Phys. J. D* **75** 229
[48] Wu Q, Teng Z and Zhu W 2022 *J. Mater. Sci.* **57** 10197
[49] Chen J L and Zhang R Q 2021 *Adv. Theory Simul.* **4** 2100022
[50] Yang Y F and Cederbaum L S 2022 *Chem. Phys. Lett.* **799** 139554
[51] Bloodworth S, Sitinova G, Alom S, Vidal S, Bacanu G R, Elliott S J, Light M E, Herniman J M, Langley G J and Levitt M H 2019 *Angew. Chem. Int. Ed.* **58** 5038
[52] Yang Y F and Cederbaum L S 2021 *Phys. Chem. Chem. Phys.* **23** 11837
[53] Jiang Y, Wu Y, Deng J and Wang Z 2021 *Phys. Chem. Chem. Phys.* **23** 8817
[54] Lide D R 2008 *CRC Handbook of Chemistry and Physics* (CRC: Boca Raton)
[55] Gutsev G L and Boldyrev A 1982 *Chem. Phys. Lett.* **92** 262
[56] Srivastava A K, Pandey S K and Misra N 2016 *Chem. Phys. Lett.* **655–656** 71
[57] Lin Z, Lu T and Ding X L 2017 *J. Comput. Chem.* **38** 1574
[58] Frisch M, Trucks G W, Schlegel H B, *et al.* 2009 *Gaussian 09*, revision D. 01. Gaussian, Inc., Wallingford CT
[59] Mayer I 1983 *Chem. Phys. Lett.* **97** 270
[60] Matito E, Poater J, Solà M, Duran M and Salvador P 2005 *J. Phys. Chem. A* **109** 9904
[61] Wang Q Q, Li P, Gao T, Wan, H Y and Ao B Y 2016 *Chin. Phys. B* **25** 063102
[62] Jacobsen H 2009 *J. Comput. Chem.* **30** 1093
[63] Yang Y 2010 *J. Phys. Chem. A* **114** 13257
[64] Dale S G and Johnson E R 2018 *J. Phys. Chem. A* **122** 9371
[65] Lu T and Chen F 2012 *J. Comput. Chem.* **33** 580
[66] Humphrey W, Dalke A and Schulten K 1996 *J. Mol. Graph. Model.* **14** 33
[67] Peng S and Zheng S 2019 *Int. J. Quantum Chem.* **119** e25942
[68] Jacquemin D, Perpete E A, Ciofini I and Adamo C 2011 *Theor. Chem. Acc.* **128** 127
[69] Malik M and Michalska D 2014 *Spectrochim. Acta A Mol. Biomol. Spectrosc.* **125** 431
[70] Thanthiriwatte K S, Hohenstein E G, Burns L A and Sherrill C D 2011 *J. Chem. Theory Comput.* **7** 88
[71] Murray J S and Politzer P 2011 *Wiley Interdiscip. Rev. Comput. Mol. Sci.* **1** 153
[72] Brinck T, Murray J S and Politzer P 1993 *J. Chem. Phys.* **98** 4305
[73] Tuer A, Krouglov S, Cisek R, Tokarz D and Barzda V 2011 *J. Comput. Chem.* **32** 1128